INELASTIC RESPONSE OF TALL STEEL FRAMES

By Masaaki Suko[I] and Peter F. Adams[II]

SYNOPSIS

A computer program has been developed to analyze steel frames with or without shear walls, which are subjected either to blast loads or to earthquake motions. Equivalent rotational springs are used at the ends of each member to account for the influence of axial load, the inelastic behavior (including the strain-hardening effect) of the member and joint distortion. The stiffness matrix is computed for the assemblage of spring connected members. The dynamic equations are solved by changing the stiffness matrix so that it is compatible with the deteriorated structure at every instant of the motion. A behavioral study presents the response of the structure to an earthquake motion.

NOTATION

The following symbols are used in this paper:

$\{B_i\}$	=	constant vector
C	=	U.D.L. term in slope deflection equations
$\{c_i\}$	=	damping coefficient (viscous damping)
D	=	U.D.L. term in slope deflection equations
E	=	modulus of elasticity
E_{st}	=	modulus in strain hardening region
I	=	moment of inertia
K	=	$\sqrt{P/EI}$
K'	=	$\sqrt{P/E_{st}I}$
K_1 .. K_8	=	coefficients in modified slope deflection equations
$[K_{ij}]$	=	stiffness matrix for the frame in terms of story shears
L	=	member length (point of inflection to the joint)

I Research Assistant, Department of Civil Engineering, University of Alberta, Edmonton.

II Associate Professor, Department of Civil Engineering, University of Alberta, Edmonton.

L_1	=	member length of elastic portion
L_2	=	member length of inelastic portion
M	=	end moment
M_{pc}	=	reduced moment capacity
M_{uc}	=	ultimate moment capacity
m_i	=	mass concentrated at i-th floor
P	=	axial load
Q	=	transverse load
$\{Q_i\}$	=	story shears
$\{R_i\}$	=	blast load distribution factor
x_i	=	floor level deflection relative to the ground
$\dot{x}_i$	=	floor level velocity relative to the ground
$\ddot{x}_i$	=	floor level acceleration relative to the ground
$\ddot{y}_o(t)$	=	ground acceleration, function of time
$Z(t)$	=	blast load, function of time
$\alpha,\beta,\gamma,\delta$	=	coefficients which express M-$\Delta\Theta$ relationship
Δ	=	deflection
Δ_e	=	elastic deflection
Δ_p	=	inelastic deflection
$\lambda_1\lambda_3$	=	rigid portion of beam
λ_2	=	flexible portion of beam
Θ	=	joint rotation
$\Delta\Theta$	=	relaxation angle
ξ	=	ratio of bottom story stiffness to top story stiffness
ρ	=	sway rotation
w	=	uniformly distributed load
ω_1	=	circular frequency in the first natural mode of undamped frame.

INTRODUCTION

The design of structural frames to resist the forces induced during an earthquake motion or blast disturbance is generally a semi-empirical procedure with the forces specified being based on dynamic analyses of simplified, idealized structures. In order to design on a more rational basis it is first necessary to have available procedures for the analysis of more complex structures (2) (3) (4) (5) (7).

The analysis presented herein has been programmed for the digital computer. The analysis traces the response of a multi-story, multi-bay structure to a dynamic disturbance resulting from a blast load or an earthquake disturbance. The inelastic behavior of the structural members is considered (including strain hardening) and the frame may contain one or more shear walls. The secondary moments produced by the vertical loads acting through the sway displacements of the frame are considered as are the influences of joint distortions or semi-rigid connections. This report describes the analytical procedure and presents a behavioral study of a series of ten-story, two-bay steel frames subjected to an earthquake motion.

ANALYTICAL PROCEDURE

The frame to be analyzed is modeled as shown in Figure 1. In the analysis the masses, m_i, are assumed to be concentrated at each floor level. Damping forces, $c_i (x_i - x_{i+1})$, are assumed to be developed by the relative motion of adjacent floors, where c_i represents the damping coefficient. A rotational spring connects every member end to the corresponding joint. The shear wall is simulated by a column which has a bending stiffness and strength equivalent to that of the original shear wall and is attached to the adjacent beams through rigid stubs. The stubs simulate the wall width effect.(8) Uniformly distributed loads are applied to the beams, although the possibility of plastic hinging within the span length of the beam is not checked. The bottom story columns are attached to the foundations by elastic rotational springs in an attempt to account for the flexibility of the foundation.

Equivalent Rotational Springs

An equivalent rotational spring is used at the ends of each member to account for the influence of axial load, the inelastic behavior (including the strain hardening effect) of the member and the joint distortion. The derivation of the spring properties will be accomplished in a series of steps.

The column shown in Figure 2 is subjected to a constant axial load, P, as well as the transverse load, Q. The moment-curvature relationship for the material and cross-section of the column is shown by the full lines in Figure 3. In Figure 3, EI represents the elastic flexural rigidity of the member and $E_{st}I$, the rigidity in the strain hardening range. M_{pc} represents the plastic moment capacity under the axial load, P, and M_{uc} the ultimate moment capacity of the member. The figure shows the correlation of the moment curvature relationship of pure bending to bending with axial load.

The deflection, Δ, at the top of the column (Figure 2), is given by:

$$\Delta = \frac{QL^3}{EI} \{\tan KL - KL\}/(KL)^3 \quad \ldots (1)$$

$$\text{for } Q \leq KM_{pc}/\tan KL \text{ (elastic behavior)}$$

$$\Delta = \Delta_e + \Delta_p \quad \ldots (2)$$

where $\Delta_e = (M_{pc} - QL_1)/P$

$$\Delta_p = \frac{Q}{P}\left(\frac{\tan K'L_2}{K'} - L_2\right) + \frac{m}{p}(\sin K'L_2 \tan K'L_2 + \cos K'L_2 - 1) \quad \ldots (3)$$

$$\text{for } Q \geq KM_{pc}/\tan KL \text{ (inelastic behavior)}$$

In the above, m represents the intercept as shown in Figure 3 and:

$$K = \sqrt{P/EI}$$

$$K' = \sqrt{P/E_{st}I} \quad \ldots (4)$$

The actual behavior of the member can be approximated by the system shown in Figure 4. The spring at the bottom of the column is forced through a rotation, $\Delta\Theta$, for the given transverse load, Q, (or the end moment, M). The spring is chosen so that the deflection at the top of the column is equal to that obtained from the solution of Equations 1 or 2, even though the axial load is eliminated. The stiffness of the column is assumed to remain equal to the elastic stiffness, EI, throughout the length, regardless of the yielded condition of the actual column.

In order to satisfy the above condition, the spring at the column base must produce a rotation, $\Delta\Theta$, for a given value of M. This rotation is given by:

$$\Delta\Theta = \frac{\Delta}{L} + \frac{ML}{3EI} \quad \ldots (5)$$

In which, Δ is the value given by either Equation 1 or Equation 2, depending upon the value of Q. The end moment is positive in a clockwise direction, therefore:

$$M = -QL \quad \ldots (6)$$

A typical M - $\Delta\Theta$ relationship is shown by the full lines in Figure 5. The dotted lines show the equivalent curves in the absence of strain hardening. This relationship is terminated when the actual moment at the bottom of the column in Figure 2 reaches the ultimate moment M_{uc}. The above relationships account for both the inelastic behavior and the axial load effect by correctly selecting the properties of the rotational springs at the ends of the member.

The connection of a member at a joint is not rigid, that is, relative rotations of the ends of the connected members will occur for example in a

bolted joint [9], as shown in Figure 6. Curve B in Figure 7 plots the relative rotation against the end moment for this situation. Also the shear deformation of the joint panel [6] [10] may cause an additional end rotation of the framing members as shown by curve C in the same figure. Curve A reproduces the M-$\Delta\Theta$ relationship of Figure 5, which includes the effects of the axial load and inelastic action. If the three M-$\Delta\Theta$ relationships, given by curves A, B, and C in Figure 7 are combined, the resulting curve is shown as curve D in Figure 7. If the spring is selected to follow this M-$\Delta\Theta$ relationship, it will be possible to approximate the effects of axial load, inelastic behavior and joint distortion by a single set of equations.

The moment-relative rotation relationship must also account for the unloading behavior. For instance, on the loading path the relative rotation may be found at point S (Figure 8) for a given moment on the curve O-A-B. Then, in order to account for the possibility of reversal of moment, the new M-$\Delta\Theta$ relationship is prepared as the line S A" B" C" (Figure 8). This method of tracing hysteresis is similar to that employed in the investigation of steel columns subjected to cyclic bending and constant axial force [1].

Slope Deflection Equations for Members Restrained by Rotational Springs

The M-$\Delta\Theta$ relationship is taken as that shown by the full lines in Figure 8, where the dashed lines show the corresponding elastic-plastic case. If such relationships are determined for member ends c and d (Figure 9), the slope deflection equations for the member, ab are modified as follows. The member is assumed to consist of rigid portions at the ends, ac and db, and a flexible portion, cd, having a stiffness EI. The relative rotation at point c, $\Delta\Theta_c$, in this deflected state, and the end moment, M_{cd}, have the relationship given by:

$$M_{cd} = \alpha(-\Delta\Theta_c) + \beta \qquad \ldots (7)$$

and similarly at point d,

$$M_{dc} = \gamma(-\Delta\Theta_d) + \delta \qquad \ldots (8)$$

and if a uniformly distributed transverse load, w, is applied over the length of the member, the end moments M_{ab} and M_{ba} are calculated as:

$$M_{ab} = \{\frac{2EI}{\lambda_3 L}(K_1\Theta_a + K_2\Theta_b + K_3\rho + K_4\frac{\beta}{\alpha} + K_5\frac{\delta}{\gamma}) + K_6 C_{cd}\}/K_7 + K_8 D_{ab} \qquad \ldots (9)$$

$$M_{ba} = \{\frac{2EI}{\lambda_3 L}(K_2\Theta_a + K_1'\Theta_b + K_3'\rho + K_5'\frac{\beta}{\alpha} + K_4'\frac{\delta}{\gamma}) + K_6' C_{dc}\}/K_7 + K_8' D_{ba} \qquad \ldots (10)$$

where

$$C_{cd} = -\frac{1}{12} w (\lambda_3 L)^2 \qquad \ldots (11)$$

$$C_{dc} = \frac{1}{12} w (\lambda_3 L)^2 \qquad \ldots (12)$$

$$K_8 D_{ab} = -\frac{1}{2} w\lambda_1 (1-\lambda_2) L^2 \quad \ldots (13)$$

$$K_8' D_{ba} = \frac{1}{2} w\lambda_2 (1-\lambda_1) L^2 \quad \ldots (14)$$

and

$$K_1 = 2+6\frac{\lambda_1}{\lambda_3} + 6\left(\frac{\lambda_1}{\lambda_3}\right)^2 + 6\frac{EI}{\gamma\lambda_3 L} + 12\frac{\lambda_1 EI}{\gamma\lambda_3^2 L} + 6\frac{\lambda_1^2 EI}{\alpha\lambda_3^3 L} + 6\frac{\lambda_1^2 EI}{\gamma\lambda_3^3 L} \quad \ldots (15)$$

$$K_1' = 2+6\frac{\lambda_2}{\lambda_3} + 6\left(\frac{\lambda_2}{\lambda_3}\right)^2 + 6\frac{EI}{\alpha\lambda_3 L} + 12\frac{\lambda_2 EI}{\alpha\lambda_3^2 L} + 6\frac{\lambda_2^2 EI}{\alpha\lambda_3^3 L} + 6\frac{\lambda_2^2 EI}{\gamma\lambda_3^3 L} \quad \ldots (16)$$

$$K_2 = 1+3\frac{\lambda_1}{\lambda_3} + 3\frac{\lambda_2}{\lambda_3} + 6\frac{\lambda_1\lambda_2}{\lambda_3^2} + 6\frac{\lambda_1 EI}{\alpha\lambda_3^2 L} + 6\frac{\lambda_2 EI}{\gamma\lambda_3^2 L} + 6\left(\frac{1}{\alpha}+\frac{1}{\gamma}\right)\frac{\lambda_1\lambda_2 EI}{\lambda_3^3 L} \quad \ldots (17)$$

$$K_3 = -(K_1+K_2) \quad \ldots (18)$$

$$K_3' = -(K_1' + K_2) \quad \ldots (19)$$

$$K_4 = 2 + 3\frac{\lambda_1}{\lambda_3} + 6\frac{EI}{\gamma\lambda_3 L} + 6\frac{\lambda_1 EI}{\gamma\lambda_3^2 L} \quad \ldots (20)$$

$$K_4' = 2 + 3\frac{\lambda_2}{\lambda_3} + 6\frac{EI}{\alpha\lambda_3 L} + 6\frac{\lambda_2 EI}{\alpha\lambda_3^2 L} \quad \ldots (21)$$

$$K_5 = 1 + 3\frac{\lambda_1}{\lambda_3} + 6\frac{\lambda_1 EI}{\alpha\lambda_3^2 L} \quad \ldots (22)$$

$$K_5' = 1 + 3\frac{\lambda_2}{\lambda_3} + 6\frac{\lambda_2 EI}{\gamma\lambda_3^2 L} \quad \ldots (23)$$

$$K_6 = 1 + 6\frac{EI}{\gamma\lambda_3 L} - \frac{6\lambda_1 EI}{\alpha\lambda_3^2 L} + 6\frac{\lambda_1 EI}{\gamma\lambda_3^2 L} \quad \ldots (24)$$

$$K_6' = 1 + 6\frac{EI}{\alpha\lambda_3 L} + 6\frac{\lambda_2 EI}{\alpha\lambda_3^2 L} - 6\frac{\lambda_2 EI}{\gamma\lambda_3^2 L} \quad \ldots (25)$$

$$K_7 = 1 + 4\left(\frac{1}{\alpha}+\frac{1}{\gamma}\right)\frac{EI}{\lambda_3 L} + 12\frac{E^2 I^2}{\alpha\gamma\lambda_3^2 L^2} \quad \ldots (26)$$

If the sway rotation, ρ, is set equal to zero in the above equations, the behavior of a beam is simulated. If

$$w = 0 \qquad \ldots (27)$$

and

$$\lambda_1 = \gamma_2 = 0;\ \lambda_3 = 1 \qquad \ldots (28)$$

are substituted, the equations simulate the action of a column.

Analysis of Complete Frame

The axial loads and points of inflection are estimated for each member in the structure. These values are then assumed to remain constant during the analysis of the frame. In calculating the moment - relative rotation relationship, the length of the equivalent cantilever, L, (Figure 2) is taken as the length from the point of inflection to the joint and the compressive load, P, is the estimated axial load for a column and zero for a beam; it is thus possible to prepare the appropriate M-$\Delta\Theta$ relationships for each member end. In the actual case the position of the points of inflection and the values of the axial load are not known beforehand and moreover may change during the loading process, consequently it is impossible to account exactly for these effects. Generally, however, these values do not change drastically during the motion of the structure, especially for the interior members of regular frames. Changes in the length, L, (Figure 2) produce relatively small changes in the M-$\Delta\Theta$ relationship, thus the M-$\Delta\Theta$ relationship is primarily a function of the axial load and the material properties.

After the M-$\Delta\Theta$ relationships have been developed for each member end, the stiffness matrix [K] , can be developed in terms of the story shears using the modified slope-deflection equations. The floor level deflection, {x}, and the story shears, {Q}, are then related by:

$$\{Q\} = [K]\{x\} + \{B\} \qquad \ldots (29)$$

In which, the vector {B} is zero vector until any portion of the structure yields, unless the gravity load produces a lateral sway.

STATIC CALCULATION

In order to check the above procedure, an analysis based on this concept has been programmed to determine the response of a given frame to a static load. The calculated results are checked against published values and are found to be reasonable. One example is given in Figure 10 [11]. The structure analyzed by Yarimci is shown in the inset. The ordinate represents the horizontal load of each floor, H, and the abscissa the sway at the first story, Δ. The solid line shows the test result and the dotted line A the theoretical calculation by Yarimci. The present calculation is compared with them by the dotted line B.

DYNAMIC EQUATIONS AND NUMERICAL SOLUTION

If the mass is assumed to be concentrated at each floor level, the dynamic equations under earthquake motion are written as follows:

$$\ddot{x}_i = -\frac{1}{m_i}\{c_i\dot{x}_i + Q_i(\{x\}) + S_i(t)\} \quad \ldots (30)$$

Where the suffixes correspond to the story number as shown in Figure 1, and,

x_i: displacement of i-th floor relative to the ground.

$\dot{x}_i$: velocity of i-th floor relative to the ground.

$\ddot{x}_i$: acceleration of i-th floor relative to the ground.

m_i: mass concentrated at i-th floor.

c_i: damping coefficient.

and $Q_i(\{x\})$ is a function of the deflected shape of the structure $\{x\}$, and represents the shear force in the i-th story, which is given by the i-th element of vector, $\{Q\}$, in Equation 29 and, $S_i(t)$ is:

$$S_i(t) = CMA_i + \ddot{y}_0(t) \times CSM_i - c_i\dot{x}_{i+1} \quad \ldots (31)$$

where $\ddot{y}_0(t)$: ground acceleration during the seismic motion

and, CMA_i and CSM_i are given by:

$$\text{for i=1 (roof):} \quad CMA_i = 0, \quad CSM_i = m_1$$

$$\text{for i=2~n-1:} \quad CMA_i = \sum_{j=1}^{i-1} m_j\ddot{x}_j, \quad CSM_i = \sum_{j=1}^{i} m_j \quad \ldots (32)$$

$$\text{for i=n (bottom):} \quad CMA_i = \sum_{j=1}^{n-1} m_j\ddot{x}_j, \quad CSM_i = \sum_{j=1}^{n} m_j$$

The evaluation of the damping effect is complex. However, it is simply assumed herein that the damping force is proportional to the relative velocity of each floor and given by:

$$c_i(\dot{x}_i - \dot{x}_{i+1}) \quad \ldots (33)$$

where c_i is chosen as:

$$c_i = 2h_iK_{ii}/\omega_1 \quad \ldots (34)$$

In this expression, K_{ii} is the i-th diagonal element of the initial stiffness matrix (Equation 29), and ω_1 is the circular frequency in the first natural mode of the undamped structure; h_i is a percentage corresponding to the percentage of critical damping used in the analysis of simple frames.

In order to solve the simultaneous, second order differential equations, such as Equation 30, the linear acceleration method is used. The response

of an example structure was computed using a time interval less than 20% of the smallest natural period of the structure, in order for the numerical integration to converge.

After finding the equilibrium position of the structure for each time interval, the end moments for every member are calculated and the member is checked to see if the end moment is compatible with the M-$\Delta\Theta$ relationship used for this state. Unless the correct choices have been made, the stiffness matrix is revised and the above procedure is repeated.

Response of Steel Frames to Earthquake Motion

Twelve, ten story two bay frames were analysed under the ground motion of the NS component of the (1940 California) El Centro earthquake scaled so that the maximum acceleration was 0.16g. The frames are classified according to the girders used as A,B, or C (See Table 1) and according to the distribution of column strength and stiffness, as A,B,C, or D (see Table 2). In Table 2, only the plastic moment capacities in the absence of axial load are listed. These capacities would be reduced in each story due to the presence of axial forces. Thus Frame AB represents a frame having type A columns and type B beams. The dimensions of the frame are shown in Figure 11; also listed in the inset of this figure, are the weights assigned to each floor level and the axial forces in the columns of each story.

The moment curavture relationships for the members of the frames are assumed to be of the shape shown in Figure 3[1], where it is assumed that $M_u = 1.2M_p = 1.2\ (\sigma_y Z)$ and $\sigma_y = 36$ ksi.

In performing the analysis, the structure is modeled as shown in Figure 1. It is assumed for these frames that no distributed loads are applied to the girders and that the column bases are fixed. The damping coefficients, h_i, are taken as 0.01. The properties of the rotational springs are computed[1] by assuming that a point of inflection forms at mid-span of each member. Typical M-$\Delta\Theta$ curves are shown, for a girder in Figure 12 and for a column in Figure 13.

The total weight of steel in each frame depends primarily on the girder weight. The total weight of the columns in the frames does not vary significantly. The period of the frame is also primarily a function of the girder stiffness. The periods for the twelve frames considered (1st mode) are listed in Table 3.

The results of the response calculations are summarized in Table 4. In Table 4, the numbers of plastic hinges to form are tabulated as well as the maximum values of the base shear coefficient, total displacement and relative story displacement for each analysis. As expected, the frame having flexible girders (Type B) develops lower base shears and is subjected to larger total displacement than the other frame. Generally speaking, however, the relative story displacements are not large and this is reflected in the relatively small amount of plastic hinging in these frames.

The behavior of Frames AA and DB, when subjected to ground motions of varying intensity, are compared in Figures 14 to 18. Figure 14 shows the locations of the inelastic regions developed during the (scaled) original

earthquake motion. Figure 15 shows the number of hinges which develop during ground motions of varying intensity. The total displacements (at the roof) are very similar for the two frames, as shown in Figure 16 but the relative story displacements are much smaller for Frame DB (flexible girders), as shown in Figure 17. The maximum base shears for this frame are also considerably lower as shown in Figure 18. As the intensity of the ground motion increases, the inelastic action is distributed throughout the building height in Frame DB, whereas for Frame AA it is localized at levels adjacent to the changes in column sections.

Summary and Conclusion

A procedure has been described for the dynamic analysis of multi-story multi-bay structures with or without shear walls. The procedure accounts for the inelastic action of the members (including strain hardening), the secondary moments produced by the axial loads and possible joint distortions in the structure.

The equilibrium equations are formulated in terms of modified slope deflection equations and the resulting stiffness matrix is modified to be compatible with the deteriorated structure at each instant of the motion. The equations of motion are formulated by assuming a linear variation of acceleration and are solved by iteration.

Dynamic analyses were performed on twelve ten-story two-bay steel frames to study the effect of variations in column stiffness distribtuion over the building height on the response.

The role of shear walls and the effect of axial loads as well as strain hardening and joint distortion will be the object of future studies using this computer program.

Acknowledgements

This study was supported by Grant No. 6301-07 provided by the Defence Research Board.

Appendix I - References

1. Akiyama, H., and Kato, B., "Inelastic Bar Subjected to Thrust and Cyclic Bending", Journal of the Structural Division, ASCE, Vol. 95, No. ST1, January 1969, pp. 33-56.

2. Clough, R.W., Benuska, K.L., and Wilson, E.L., "Inelastic Earthquake Response of Tall Buildings", Proceedings, Third World Conference on Earthquake Engineering, Wellington, New Zealand 1965, pp. II-68-89.

3. Clough, R.W., and Benuska, K.L., "Nonlinear Earthquake Behavior of Tall Buildings", Journal of the Engineering Mechanics Division, ASCE, Vol. 93, No. EM3, June 1967, pp. 129-146.

4. Goel, S.C., and Berg, G.V., "Inelastic Earthquake Response of Tall Steel Frames", Journal of the Structural Division", ASCE, Vol. 94, No. ST8, August 1968, pp. 1907-1934.

5. Goel, S.C., "P-Δ and Axial Column Deformation in Aseismic Frames", Journal of the Structural Division, ASCE, Vol. 95, No. ST8, August 1969, pp. 1693-1711.

6. Jensen, C.D., et al, "Welded Interior Beam-to-Column Connections", A.I.A. File No. 13-C, American Institute of Steel Construction, Inc., 1959.

7. Lionberger, S.R., and Weaver, W., Jr., "Dynamic Response of Frames with Nonrigid Connections", Journal of the Engineering Mechanics Division, ASCE, Vol. 95, No. EM1, February 1969, pp. 95-114.

8. Michael, D., "The Effect of Local Wall Deformations on the Elastic Interaction of Cross Walls Coupled by Beams", Tall Buildings, Proceedings of the Symposium held at the University of Southampton, Pergamon Press Ltd., April 1966, pp. 253-272.

9. Munse, W.H., Bell, N.G., and Cherson, E., Jr., "Behaviour of Beam-to-Column Connections", Transactions, ASCE, Vol. 126, Part II, 1961, pp. 729-749.

10. Naka, T., et al, "Static and Dynamic Behavior of Steel Beam-to-Column Connections", Yawata Technical Report, No. 256, Yawata Iron and Steel Co. Ltd., September 1966, pp. 98-113, and pp. 263-266.

11. Yarimci, E., "Incremental Inelastic Analysis of Framed Structures and Some Experimental Verifications", Fritz Engineering Laboratory Report, No. 273.45, Lehigh University, 1966.

Beam Type	Moment of Inertia (in^4)	Plastic Moment Capacity (in-K)	Section
A	1141	4401	21WF55
B	344	2551	10WF59
C	516	2574	16WF41

TABLE 1

PROPERTIES OF BEAMS

Column Type	Story	Moment of Inertia (in^4)	Plastic Moment Capacity (in-K)	Section
A	1-3	110	1032	8WF31
	4-6	334	2551	10WF59
	7,8	723	4464	12WF85
	9,10	931	5677	12WF106
B	1-6	344	2551	10WF59
	7-10	723	4464	12WF85
C	1-10	533	3342	Properties do not correspond to existing sections.
D	1	408	2592	
	2	433	2743	
	3	458	2893	
	4	483	3042	
	5	508	3192	
	6	533	3342	
	7	558	3490	
	8	583	3639	
	9	608	3787	
	10	633	3935	

TABLE 2

PROPERTIES OF COLUMNS

(sec)

Beam / Column	A	B	C
A	2.39	3.42	2.99
B	2.33	3.39	2.95
C	2.34	3.42	2.96
D	2.31	3.38	2.93

TABLE 3

UNDAMPED NATURAL PERIOD (1st MODE)

a) Number of Plastic Hinges

Beam / Column	A	B	C
A	13	2	14
B	10	1	7
C	8	4	9
D	10	1	9

b) Maximum Base Shear Coefficient

Beam / Column	A	B	C
A	.115	.065	.076
B	.108	.059	.081
C	.073	.054	.064
D	.091	.059	.077

c) Maximum Roof Displacement (in)

Beam / Column	A	B	C
A	9.7	12.4	11.3
B	8.9	12.0	11.2
C	6.9	11.7	10.8
D	8.0	11.8	11.5

d) Maximum Relative Storey Displacement (in)

Beam / Column	A	B	C
A	3.05 (3)	1.80 (3)	2.61 (3)
B	1.37 (6)	1.71 (6)	1.82 (6)
C	1.29 (10)	1.64 (8)	1.78 (9)
D	1.45 (9)	1.64 (8)	1.55 (8)

*The numbers in brackets represent the story where maximum displacement occurred.

TABLE 4

RESPONSE TO EL CENTRO EARTHQUAKE, MAY 1940

NS COMPONENT, MAXIMUM ACCELERATION = .16G

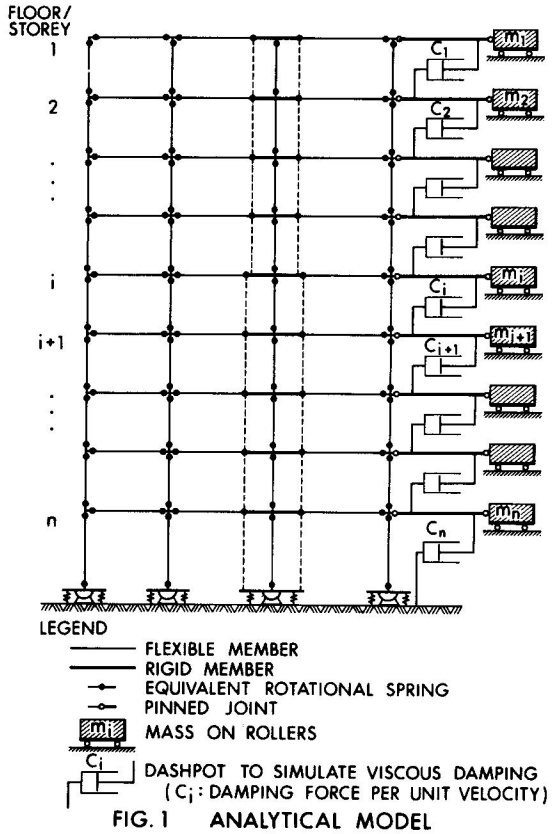

FIG. 1 ANALYTICAL MODEL

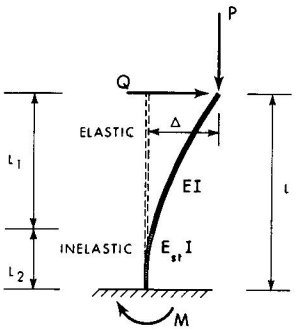

FIG. 2 COLUMN WITH AXIAL LOAD

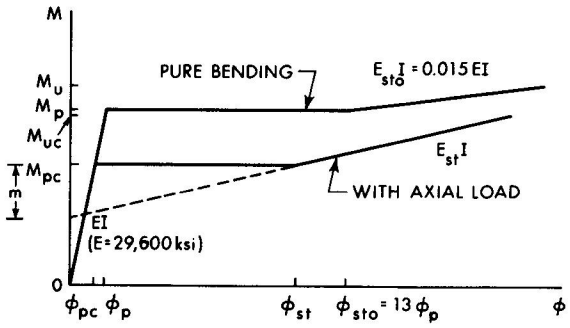

FIG. 3 MOMENT-CURVATURE RELATIONSHIP

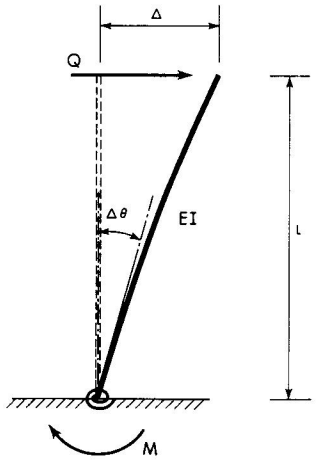

FIG. 4 RESTRAINED COLUMN

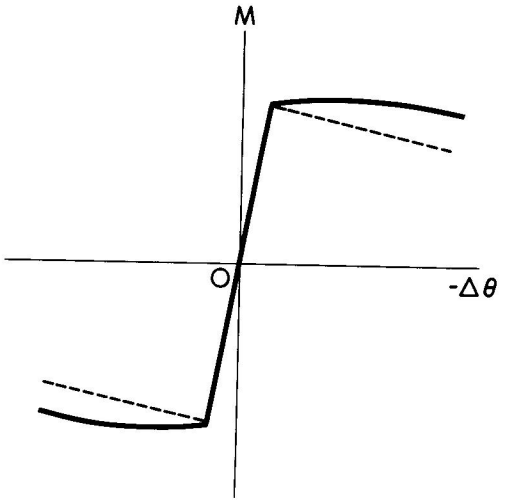

FIG. 5 M-Δθ RELATIONSHIP

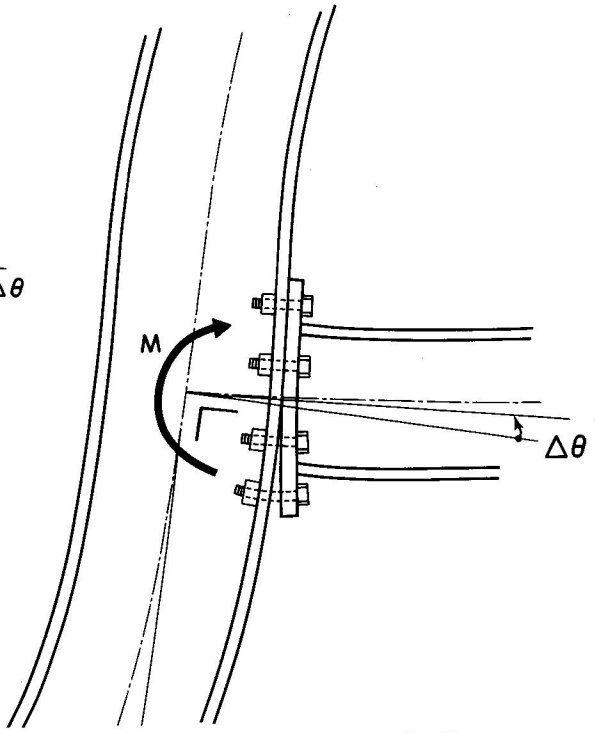

FIG. 6 SEMI-RIGID JOINT

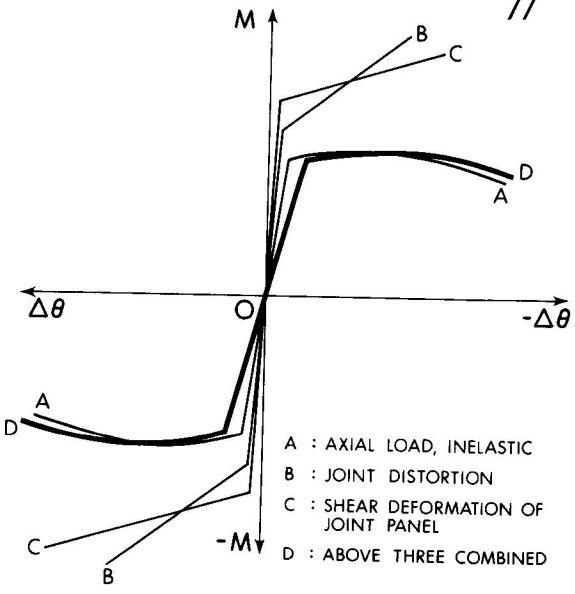

FIG. 7 M-Δθ RELATIONSHIP

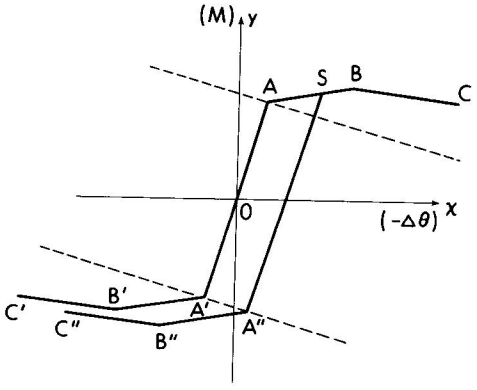

FIG. 8 IDEALIZED M-Δθ RELATIONSHIP

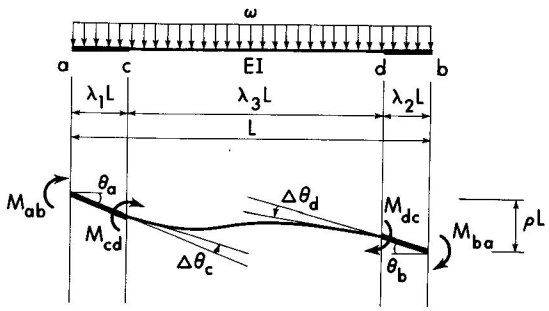

FIG. 9 RESTRAINED MEMBER

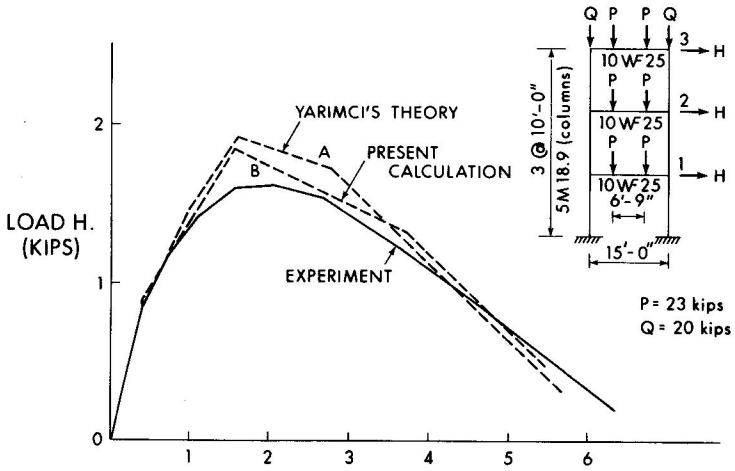

FIG. 10 STATIC RESPONSE

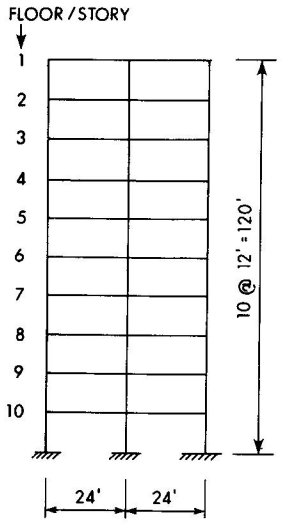

WEIGHT (KIPS)	COLUMN AXIAL LOADS (KIPS)	
	EXTERIOR	INTERIOR
60 (60)*	18.0	24.0
105 (165)	49.5	66.0
105 (270)	81.0	108.0
105 (375)	112.5	150.0
105 (480)	144.0	192.0
105 (585)	175.5	234.0
105 (690)	207.0	276.0
105 (795)	238.5	318.0
105 (900)	270.0	360.0
105 (1005)	301.5	402.0

*THE VALUES IN BRACKETS REPRESENT CUMULATIVE WEIGHTS

FIG. 11 EXAMPLE FRAME

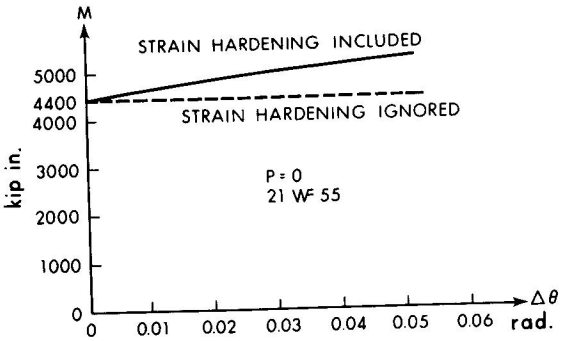

FIG. 12 M-Δθ RELATIONSHIP-BEAMS - TYPE A

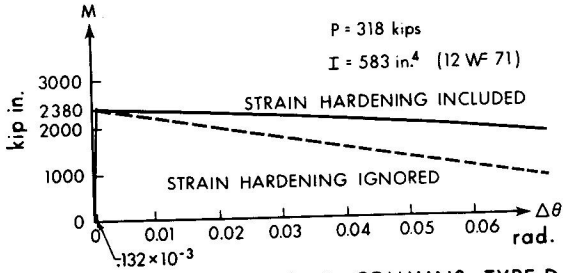

FIG. 13 M-Δθ RELATIONSHIP - COLUMNS - TYPE D

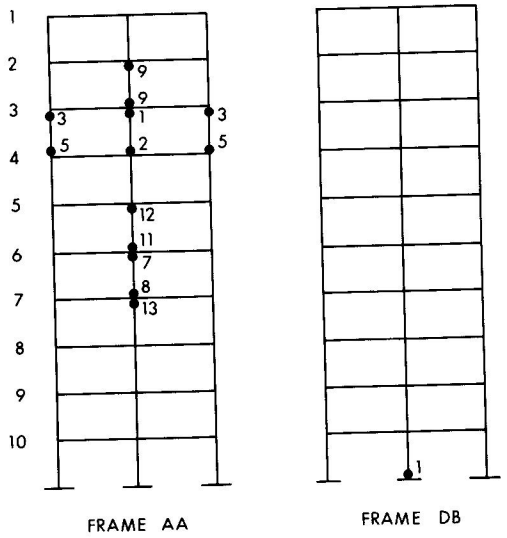

MAXIMUM ACCELERATION 0.16 g

FIG. 14 LOCATION OF PLASTIC HINGES

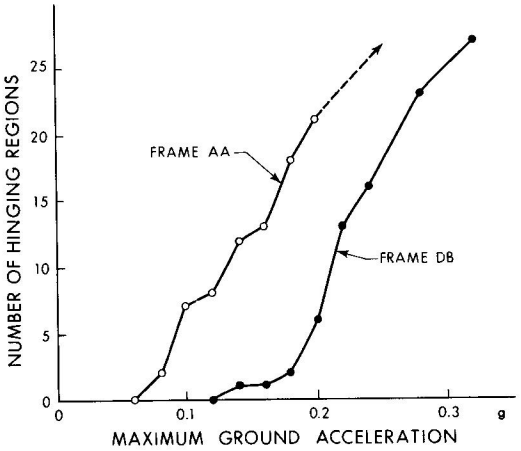

FIG. 15 NUMBER OF PLASTIC HINGES

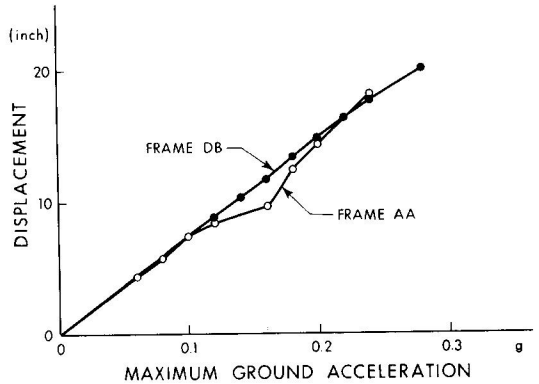

FIG. 16 DISPLACEMENT AT ROOF LEVEL

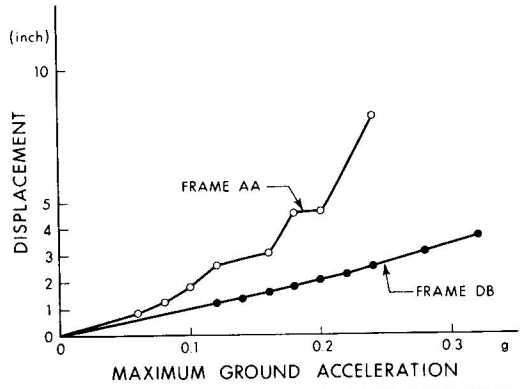

FIG. 17 RELATIVE STORY DISPLACEMENT

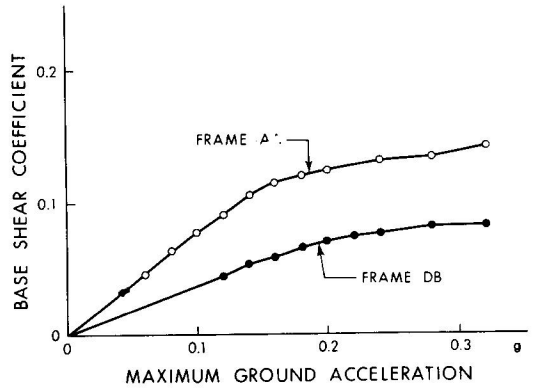

FIG. 18 BASE SHEAR COEFFICIENT